J Mater Sci (2011) 46:2179–2184
DOI 10.1007/s10853-010-5055-6

Synthesis of copper oxide vegetable sponges and their antibacterial, electrochemical and photocatalytic performance

L. J. Xie · W. Chu · J. H. Sun · P. Wu · D. G. Tong

Received: 20 August 2010 / Accepted: 3 November 2010 / Published online: 23 November 2010

Abstract Copper oxide (CuO) vegetable sponges with mesoporous structure were successfully prepared from pine tree needles cellulose as templates. The sample was characterized by X-ray diffraction, scanning electron microscopy and nitrogen absorption–desorption. In the performance test, the obtained CuO vegetable sponges showed great antibacterial activities, as good as penicillin and kanamycin, especially towards *Streptococcus faecalis*. They also displayed active photocatalytic degradation of rhodamine B molecules in aqueous solution. Electrochemical data demonstrated that the CuO vegetable sponges were capable of delivering a specific capacitance of 440 F g^{-1} at a current density of 1 A g^{-1} and offered good specific capacitance retention of 95.1% after 1,000 continuous charge–discharge cycles even at 5 A g^{-1}.

Introduction

Copper oxide (CuO) is an important material and has been recognized as being used in preparing high temperature superconductors, magneto resistance materials, catalysts in many organic reactions, and anode materials for Li ion batteries [1, 2]. Therefore, the synthesis and the application study of CuO have both theoretical and practical importance. Because the properties of materials are strongly influenced by their morphology, numerous works have investigated the morphology and property of CuO [3]. Up to now, CuO with different morphologies, such as nanorods, nanotubes, hollow microsphere, microflower, aligned nanowires, and dandelion, have been successfully synthesized and studied [3–8]. It is evident that the purpose of preparing CuO in various shapes has been driven by the strong interest in their novel properties and potential applications.

Nature provides a multiplicity of materials, architectures, systems and functions with many inspiring properties such as sophistication, miniaturization, hierarchical organizations, adaptability and environmental response [9]. Mimicking the elaborate architectures to prepare more reliable and efficient materials is highly appealing.

In this article, we prepared CuO vegetable sponges with mesoporous structure by using pine tree needles cellulose as templates in air for the first time. The antibacterial activities, electrochemical properties, and photocatalytic performance of the as-prepared sample were investigated.

Experimental

Preparation of CuO vegetable sponges

All chemicals were analytical grade and were used without further purification. Fresh pine tree needles were treated with 5% glutaraldehyde/phosphate buffer solution (pH 7) under 4 °C for 12 h for the fixation of cells and tissues. Then the samples were rinsed with pure water and treated with 10% HCl solution for 12 h. After rinsing with pure water, the pine tree needles cellulose was obtained.

The obtained cellulose was stressed with 0.2 mol L^{-1} $Cu(NO_3)_2$ solution in oven at 120 °C for 12 h. Then the

L. J. Xie · W. Chu (✉) · D. G. Tong
College of Chemical Engineering, Sichuan University, Chengdu 610065, China
e-mail: chuwei65@yahoo.com.cn

J. H. Sun · P. Wu · D. G. Tong (✉)
College of Materials and Chemistry and Chemical Engineering, Chengdu University of Technology, Chengdu 610059, China
e-mail: tongdongge@163.com

mixture was rinsed with pure water and following infiltrated in 0.8 mol L^{-1} $Cu(NO_3)_2$ solution in an oven at 60 °C for 72 h. After being desiccated in an oven at 80 °C for 8 h, the sample was calcined in air at 400 °C for 2 h.

A common CuO sample was prepared via a similar process that described above without using pine tree needles cellulose and was designated CuO-common.

Characterization

The samples were characterized by scanning electron microscopy (SEM, JEOL/EO, JSM-5900), X-ray powder diffraction using Cu K_α sources (XRD, Philips, XPERT-PRO), and N_2 adsorption–desorption. The UV–vis absorption spectra of the samples dispersed in water were taken on a Shimadzu UV–vis scanning spectrometer (Model 2101 PC).

The antibacterial activities of the samples were tested against *Bacillus subtilis* (*B. subtilis*), *Staphylococus aureus* (*S. aureus*), *Streptococcus faecalis* (*S. faecalis*), *Pseudomonas aeruginosa* (*P. aeruginosa*) and *Enterobacter cloacae* (*E. cloacae*) by determining the minimum inhibitory concentrations (MICs, μg mL^{-1}) through a colorimetric method using the dye MTT according to the method referenced to the reported literature [10].

Photocatalytic experiments were carried out in a homemade photoreactor, containing the required quantity of samples and rhodamine B (RhB) aqueous solution. The suspension was irradiated with a 300 W high pressure mercury lamp. The reaction suspension was prepared by adding the sample (0.6 g L^{-1}) into 400 mL of RhB solution (20 mg L^{-1}). The suspension was stored in the dark and stirred for 30 min to ensure an adsorption/desorption equilibrium prior to reaction. The concentration of RhB in the solution was determined using a UV-3000 spectrophotometer by collecting the absorbance of RhB at 553 nm.

CuO electrodes were formed by 85 wt% active material, 10 wt% acetylene black and 5 wt% polytetrafluoroethylene (PTFE). Mixture was pressed on Ni-foam (1 × 1 cm). The electrochemical measurements were carried out by means of an electrochemical analyzer system, CHI660B (Chenhua, Shanghai, China) in a three-electrode arrangement. The prepared electrode was used as working electrode, a nickel plate as counter electrode, and saturated calomel electrode (SCE) as reference electrode. The electrolyte was a 6 mol L^{-1} KOH solution.

Results and discussion

Morphologies of the pine tree needles cellulose (Fig. 1a) and the prepared CuO vegetable sponges were studied by SEM. Obviously, CuO duplicates the morphology of pine tree needles cellulose (Fig. 1b). At high magnification SEM image (Fig. 1c), we can see that the microstructure of the CuO vegetable sponges is built from nanoparticles. These uniform nanoparticles were connected to each other and formed the porous structure (Fig. 1c). We found that the pine tree needles cellulose played a crucial role during the formation CuO vegetable sponges. Without cellulose, only the common CuO with irregular morphologies was obtained (Fig. 1d).

The formed mesoporous structure of CuO vegetable sponges is confirmed by N_2 adsorption–desorption isotherm. The isotherm (Fig. 2a) showed a typical IUPAC type pattern with inflection of N_2 adsorbed at P/P_0 about 0.50 (type H_2 hysteresis loop) [11], indicating the presence of mesopores. The pore size distribution (Fig. 2b) shows that CuO vegetable sponges had a broad pore size distribution in the range of 3–43 nm. Its average pore diameter was about 6.7 nm. The specific surface area was 84.52 m^2/g. It is much larger than that of common CuO nanoparticles (6.57 m^2/g) [12].

Figure 2c shows the XRD patterns of the as-prepared sample. All of the diffraction peaks can be clearly indexed as the monoclinic phase of CuO (JCPDS card no. 80-1917). No impurity peaks are observed, indicating a high purity of the product.

Based on the above results, the formation of CuO vegetable sponges can be simply described in Fig. 2d. In the initial stage of copper nitrate solution infiltration, NO_3^- and Cu^{2+} were attracted to the polar groups such as the hydroxyl, carboxylic and ester radicals, which are located on the surface of the cellulose. During drying, the surface of cellulose was covered with NO_3^- and Cu^{2+}. When the precursor was subjected to calcination at 400 °C in air, the decomposition of NO_3^- together with the thermal degradation of cellulose took place. Volatile species like H_2O and carbonyls were released, and carbon in the cellulose was further oxidized to form carbon dioxide [9]. The gaseous CO_2 molecules diffused out from the cellulose templates. At the same time, CuO nanoparticles were formed. Guided by the cellulose templates, these nanoparticles connected to form vegetable sponges microstructure.

CuO has wide applications in many fields, however, little literature has reported its antimicrobial activities [12]. In this study, we studied the antimicrobial activities of CuO vegetable sponges against *B. subtilis*, *S. aureus*, *S. faecalis*, *P. aeruginosa* and *E. cloacae* (Table 1). For comparison, the MICs of penicillin and kanamycin to the five bacteria are also presented. The results demonstrate that the CuO vegetable sponges can kill all of the tested bacteria well, especially *S. faecalis*, while the commercial CuO (Kexi, 99.99%) with sizes in the range of 50–100 nm (Fig. 1e) and the CuO-common prepared in this work without

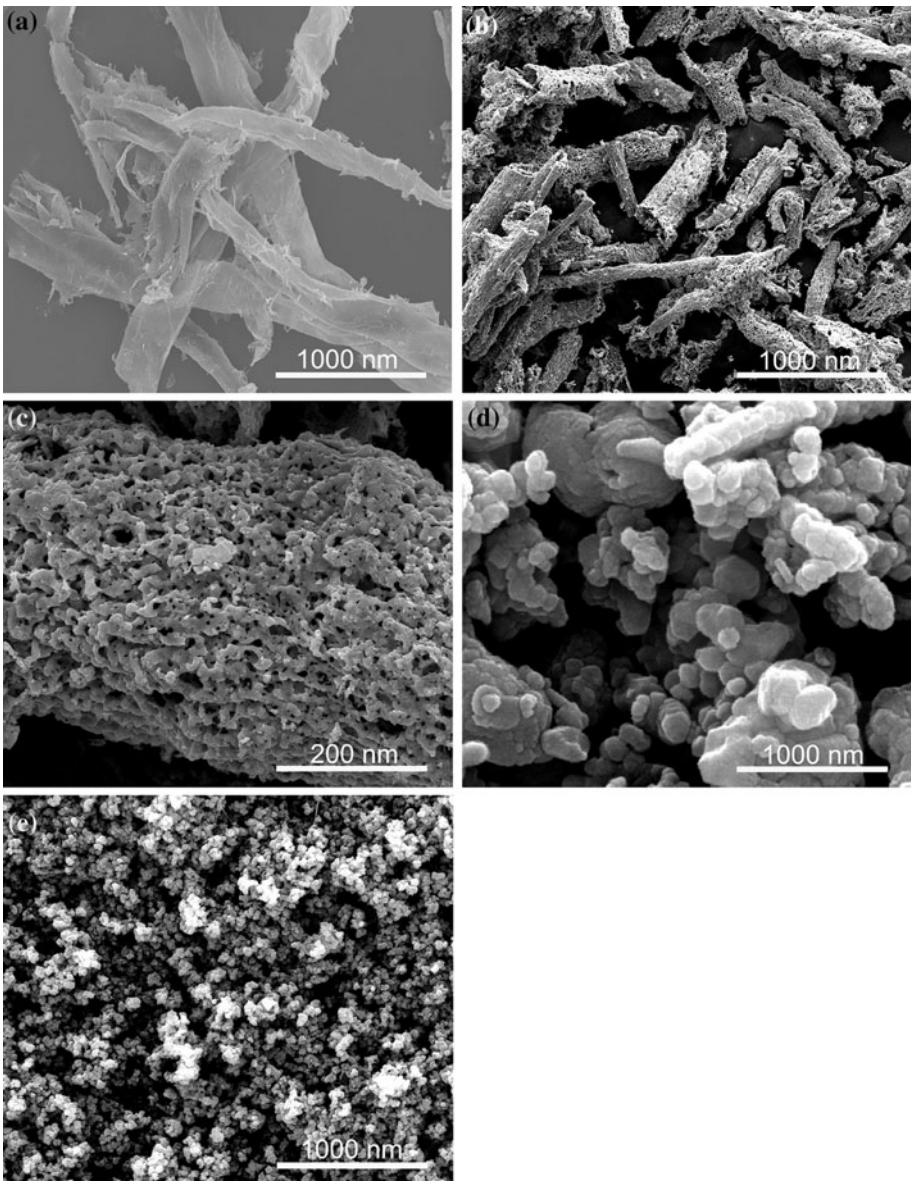

Fig. 1 SEM images of **a** pine tree needles cellulose, **b** and **c** CuO vegetable sponges at different magnifications, **d** CuO-common and **e** commercial CuO

cellulose have no or very weak antibacterial abilities to the tested five bacteria. Although the real mechanism of the antibacterial effect is still uncertain, there is no doubt that this effective antibacterial ability of CuO vegetable sponges would arise from their special structure (Fig. 1b, c), in which their interior might inhibit the growth of bacterial and the high specific surface area would increase the efficiency of antimicrobial performance [12]. In other words, the effective antimicrobial activity of CuO vegetable sponges enable them to be applied in the range from the coating of medical devices to the direct treatment of wounds or burns.

The energy band structure feature of a semiconductor is considered as a key factor to determinate its photocatalytic activity [13]. Figure 3a shows the UV–vis spectrum of CuO vegetable sponges dispersed in water. The strong absorption in the UV region observed at 375 nm is attributed to band gap absorption in CuO [14]. It is well known that optical band gap (E_g) can be calculated on the basis of the optical absorption spectrum by the following equation (1):

$$(Ah\upsilon)^n = K(h\upsilon - E_g), \quad (1)$$

where $h\upsilon$ is the photo energy, A is the absorbance, K is a constant relative to the material and n depends on the characteristics of the transition in a semiconductor [15]. For CuO, the value of n is 2 for the direct transition. The optical band gap of CuO vegetable sponge was 2.61 eV estimated by extrapolating the linear portion of the $(Ah\upsilon)^2$–$h\upsilon$ curve to zero (Fig. 3b), which was larger than the reported value for the bulk CuO (1.20 eV), due to the quantum confinement effects [16].

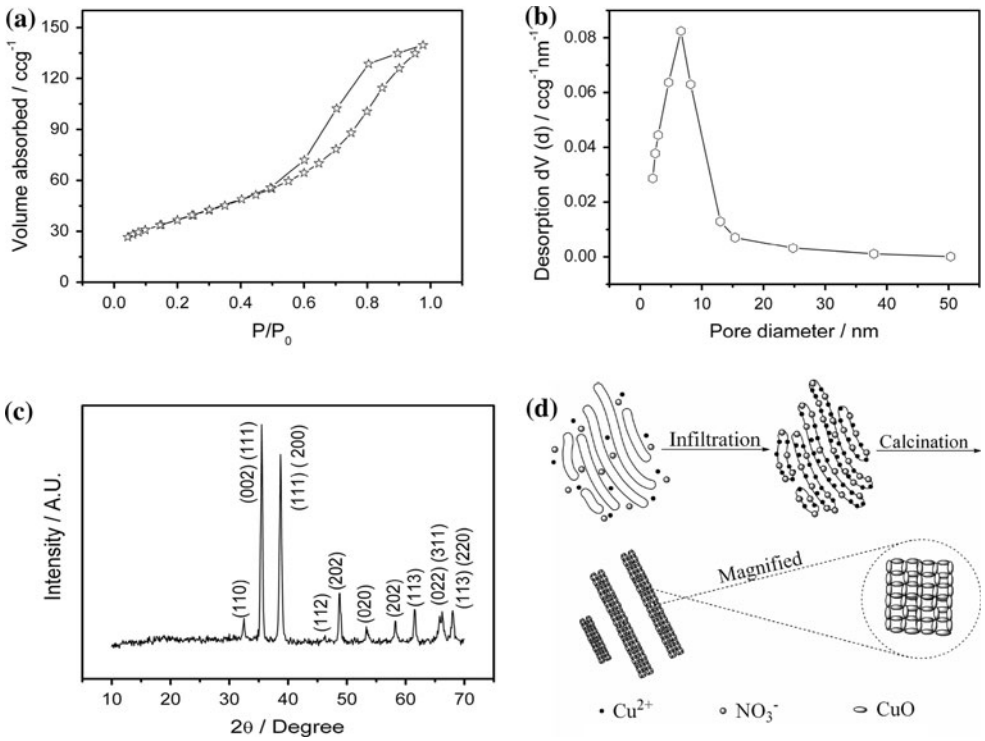

Fig. 2 **a** N_2 adsorption–desorption curves, **b** pore size distribution, **c** XRD pattern and **d** the formation scheme of CuO vegetable sponges

Table 1 Antibacterial activities of the samples

Samples	Minimum inhibitory concentration (μg mL^{-1})				
	Gram positive			Gram negative	
	B. subtilis	*S. aureus*	*S. faecalis*	*P. aeruginosa*	*E. cloacae*
CuO vegetable sponges	10.263	4.892	1.589	8.243	7.560
CuO-common	45.709	61.892	39.432	53.423	49.546
Commercial CuO	52.546	57.803	47.845	31.234	25.326
Kanamycin	0.381	1.602	3.223	3.223	1.602
Penicillin	1.602	1.602	1.602	6.201	3.223

In order to evaluate the photocatalytic activities of the as-prepared CuO vegetable sponges, decolorization of RhB solution under visible light irradiation was studied. Figure 3c shows UV–vis adsorption spectra of RhB as a function of irradiation time using CuO vegetable sponges as photocatalysts, indicating that the synthesized sample has remarkable photocatalytic ability. After 60 min irradiation, RhB molecules have been degraded to a level of 95%, while without the addition of the CuO vegetable sponges, RhB is almost unchanged (Fig. 3d). We also used the commercial CuO and the CuO-common as references to evaluate the photocatalytic performance of CuO vegetable sponges. After irradiation for 60 min, the degradation of RhB over the commercial CuO and the CuO-common are 37 and 22%, respectively. The great photocatalytic activities of CuO vegetable sponges should be due to their large surface area and the unique mesoporous structure, which can facilitate mass transfer and increase the accessibility of active sites on CuO surface to RhB molecules [11, 17–20].

Figure 4 shows the cyclic voltammogram of CuO vegetable sponges at a scan rate of 5 mV s^{-1}. A quasi-perfect rectangular shaped voltammogram with a large current separation was observed. It indicated that CuO vegetable sponges are suitable for electrochemical capacitor applications [21]. The nonlinear charge–discharge curves (Fig. 4b) further verify the pseudocapacitance. The discharge specific capacitance of the sample was calculated from the discharge curve based on Eq. 2. In Eq. 2, C, I, t and ΔV are the specific capacitance (F g^{-1}) of the CuO

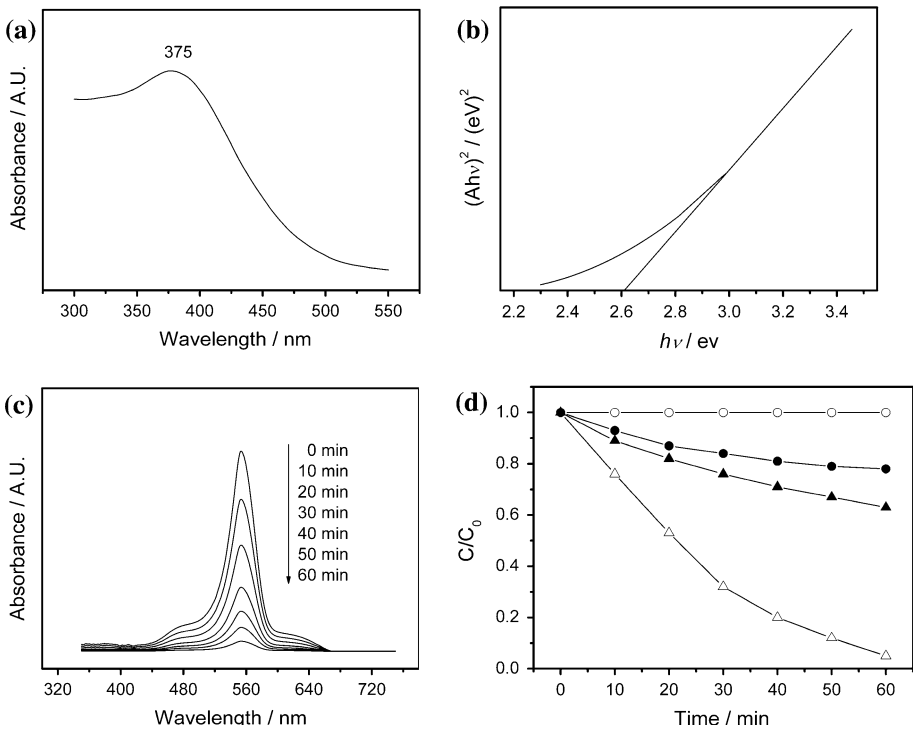

Fig. 3 **a** UV–vis absorption spectrum of CuO vegetable sponges dispersed in water, **b** $(Ahv)^2$ vs. (hv) curves, **c** UV–vis adsorption spectra of rhodamine B as a function of irradiation time using CuO vegetable sponges as photocatalysts, **d** a plot of the photodegradation extent of rhodamine B molecules as a function of irradiation time for the blank (*circle*), CuO vegetable sponges (*square*), CuO-common (*filled circle*) and commercial CuO (*filled triangle*)

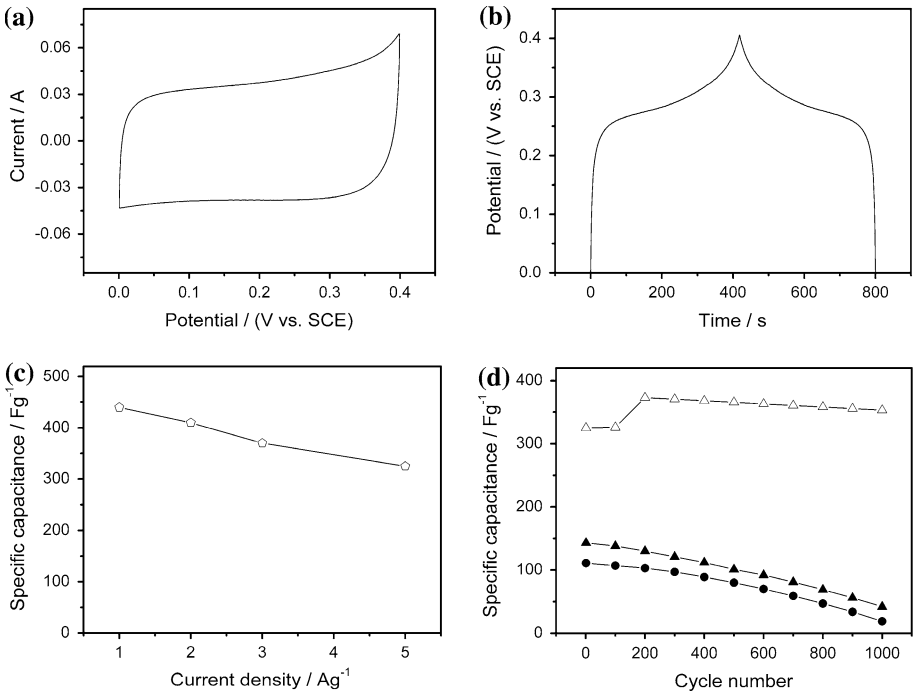

Fig. 4 **a** Cyclic voltammogram at a scanning rate of 5 mV s^{-1}, **b** charge–discharge curve at a current density of 1 A g^{-1}, **c** specific capacitance as a function of the current density, **d** specific capacitance as a function of cycle number for CuO vegetable sponges (*square*), CuO-common (*filled circle*) and commercial CuO (*filled triangle*)

vegetable sponges electrode, the discharging current density (A g^{-1}), the discharging time (s) and the discharging potential range (V), respectively.

$$C = (I * t)/\Delta V \quad (2)$$

The calculated specific capacitance of CuO vegetable sponges is 440 F g^{-1} at a current density of 1 A g^{-1}. Considering the different price between RuO_2 and CuO, this value is satisfactorily comparable to that reported for electroactive RuO_2 [22, 23]. Impressively, the unique CuO vegetable sponges not only exhibited high specific capacitance, but also excellent cycle stability. It preserved more than 74% of their specific capacitance delivered at 1 A g^{-1} as the current density increased to 5 A g^{-1} (from 440 to 325 F g^{-1}), as shown in Fig. 4c. This result indicates that

CuO vegetable sponges can serve as a good electroactive material for electrochemical capacitors, due to their ability to provide high power and maintain a promising energy density at a high charge/discharge rate.

Figure 4d shows the cycle performance for CuO vegetable sponges at a current density of 5 A g^{-1} within a voltage range between 0.0 and 0.4 V in 6 mol L^{-1} KOH electrolyte. During the first 200 cycles, the specific capacitance increased from 325 to 373 F g^{-1}. It is due to the activation process of CuO vegetable sponges during cycling. Thereafter, it decreased to 355 F g^{-1} after the subsequent 800 continuous cycles. The capacitance degradation is only 4.9%. For the commercial CuO and the CuO-common, the initial specific capacitances were 143 and 111 F g^{-1}, respectively. After 1,000 cycles, the specific capacitances of the commercial CuO and the CuO-common dropped to 82.1 and 70.7% of the initial values, respectively.

The excellent electrochemical performance of CuO vegetable sponges can be attributed to their unique structure with rich diffusion pores, which reduce the diffusion lengths for the electrolyte ions and ensure the thoroughly contact with enough electrolyte ions [24–28]. In addition, such a sponge structure, due to its 'ion-buffering reservoirs', could offer a robust sustentation of electrolyte ions and ensure that sufficient electrochemical reactions can take place at high current densities for energy storage [24–28]. This in turn would ensure better utilization and higher-rate charge/discharge performance.

Conclusions

In summary, CuO vegetable sponges have been successfully synthesized by using pine tree needles cellulose as templates. The obtained CuO vegetable sponges showed great antibacterial activities, as good as penicillin or kanamycin, especially towards *S. faecalis*. They also display active photocatalytic function on the decolorization of RhB aqueous solution. Electrochemical data demonstrated that the CuO vegetable sponges could deliver 373 F g^{-1} even at a current density of 5 A g^{-1} and offer lower specific capacitance degradation of 4.9% after 1,000 cycles. This indicates that we successfully met key requirements in terms of large specific energy density, high-rate capability and good electrochemical stability. We believe that research of the bacteriostatic effect, the photocatalytic activity and the electrochemical performance of CuO vegetable sponges are useful, which may be expected to lead to their use in a number of applications that involve nano-biomaterial, catalysis, electrochemical supercapacitor and so forth.

References

1. Schon JH, Dorget M, Beuran FC, Zu XZ, Arushanov E, Cavellin CD (2001) Nature 414:434
2. He LF, Jia Y, Meng FL, Li MQ, Liu JH (2009) J Mater Sci 44:4326. doi:10.1007/s10853-009-3645-y
3. Liu B, Zeng HC (2004) J Am Chem Soc 126:8124
4. Cao MH, Hu CW, Wang YH, Guo YH, Guo CX, Wang EB (2003) Chem Commun 15:1884
5. Wang WZ, Zhan YJ, Wang GH (2001) Chem Commun 13:727
6. Zhang YG, Wang ST, Qian YT, Zhang ZD (2006) Solid State Sci 8:462
7. Xu YY, Chen DR, Jiao XL, Xue KY (2007) Mater Res Bull 42:1723
8. Kaur M, Muthe KP, Despande SK, Choudhury S, Singh JB, Verma N (2006) J Cryst Growth 289:670
9. Fan TX, Chow SK, Zhang D (2009) Prog Mater Sci 54:542
10. Meletiadis J, Meis JF, Mouton JW, Donnelly JP, Verweij PE (2000) J Clin Microbiol 38:2949
11. Xu RE, Pang WQ, Yu JH, Hu QS, Chen JS (2004) Chemistry of molecular sieve and porous materials. Science Press, Beijing
12. Gao F, Pang H, Xu SP, Lu QY (2009) Chem Commun 21:3571
13. Tang JW, Zou ZG, Ye JH (2004) Angew Chem Int Ed 43:4463
14. Xu XD, Zhang M, Feng J, Zhang ML (2008) Mater Lett 62:2787
15. Tsunekawa S, Fukuda T, Kasuya A (2000) J Appl Phys 87:1318
16. Zhu JW, Chen HQ, Liu HB, Yang XJ, Lu LD, Wang X (2004) Mater Sci Eng A 384:172
17. Tong DG, Chu W, Luo YY, Chen H, Ji XY (2007) J Mol Catal A 269:149
18. Tong DG, Han Y, Chu W, Chen H, Ji XY (2007) Mater Lett 61:4679
19. Tong DG, Han Y, Chu W, Chen H, Ji XY (2008) Mater Res Bull 43:1327
20. Tong DG, Zeng XL, Chu W, Wang D, Wu P (2010) J Mater Sci 45:2862. doi:10.1007/s10853-010-4275-0
21. Conway BE (1999) Electrochemical supercapacitors scientific fundamentals and technological applications. Kluwer/Plenum Publishers, New York
22. Liu R, Huberb TA, Kopacb MC, Pickupa PG (2009) Electrochim Acta 54:7141
23. Mina CK, Wu TB, Yang WT, Li CL (2009) Mater Chem Phys 117:70
24. Yuan CZ, Chen L, Gao B, Su LH, Zhang XG (2009) J Mater Chem 19:246
25. Wu MS, Huang YA, Yang CH (2009) J Electrochem Soc 155:A798
26. Zhang HX, Feng J, Zhang ML (2008) Mater Res Bull 43:3221
27. Tong DG, Chu W, Zeng XL, Tian W, Wang D (2009) Mater Lett 63:1555
28. Tong DG, Wang D, Chu W, Sun JH, Wu P (2010) Electrochim Acta 55:2299